þÿProton pumping by cytochrome c oxidase : A 40/

Wikström, Mårten

2018-09

þÿWikström , M & Sharma , V 2018 , ' Proton pumping by cytochrome c ox
anniversary ' , Biochimica et Biophysica Acta. Bioenergetics , vol. 1859 , no. 9 , pp. 692-698
. https://doi.org/10.1016/j.bbabio.2018.03.009

http://hdl.handle.net/10138/300200
https://doi.org/10.1016/j.bbabio.2018.03.009

Proton pumping by cytochrome c oxidase – A 40 year anniversary

Mårten Wikström, Vivek Sharma

PII: S0005-2728(18)30042-2
DOI: doi:10.1016/j.bbabio.2018.03.009
Reference: BBABIO 47889

To appear in:

Received date: 8 March 2018
Accepted date: 14 March 2018

Please cite this article as: Mårten Wikström, Vivek Sharma , Proton pumping by cytochrome c oxidase – A 40 year anniversary. The address for the corresponding author was captured as affiliation for all authors. Please check if appropriate. Bbabio(2018), doi:10.1016/j.bbabio.2018.03.009

BBA/EBEC Special Issue 2018

Proton pumping by cytochrome *c* oxidase – a 40 year anniversary

Mårten Wikström[1] and Vivek Sharma[1,2]

[1]Institute of Biotechnology, University of Helsinki, P.O. Box 56, Helsinki 00014, Finland

[2]Department of Physics, University of Helsinki, P.O, Box 64, Helsinki 00014, Finland

ABSTRACT

Cytochrome *c* oxidase is a remarkable energy transducer that seems to work almost purely by Coulombic principles without the need for significant protein conformational changes. In recent years it has become possible to follow key partial reactions of the catalytic cycle in real time, both with respect to electron and proton movements. These experiments have largely set the stage for the proton pump mechanism. The structures of the catalytic binuclear heme-copper site that is common to the huge family of heme-copper oxidases, are today well understood throughout the catalytic cycle of oxygen reduction to water based on both spectroscopic studies and quantum chemical calculations. Here, we briefly review this progress, and add some recent details into how the proton pump mechanism is protected from failure by leakage.

1. Introduction

Cytochrome *c* oxidase is the terminal enzyme complex of the respiratory chain (complex IV) in all mitochondria and in several aerobic bacteria (Fig. 1). It is responsible for catalysing the final step of cell respiration, i.e. the activation and reduction of O_2 to water with the help of reducing equivalents derived from the oxidation of foodstuffs via NAD and complexes I and III of the chain. Together with complexes I and III, cytochrome *c* oxidase harnesses a considerable proportion of the free energy of the catalysed redox reaction, and transduces it into an electrochemical proton gradient (protonmotive force, pmf) across the inner mitochondrial or bacterial plasma membrane. As is generally known today, the electrochemical proton gradient is the driving force for secondary energy transduction, viz. for the synthesis of ATP from ADP and inorganic phosphate by the F_1F_o ATP synthase, and for a number of ion and metabolite transport systems, the functions of which are driven by either or both of the components of the protonmotive force, the electrical membrane potential and the pH gradient. This chemiosmotic principle of energy transduction in biology, proposed by Peter Mitchell (1), extends to the energy transduction processes of photosynthesis, and is thus truly universal.

Originally, the chemiosmotic view of cytochrome *c* oxidase function (1) was that it would complete the last ”redox loop” of the respiratory chain by transferring electrons from cytochrome *c* on the outer positively charged surface (***P***-side) of the inner mitochondrial membrane, inwards across the membrane to the active site of O_2 reduction. Here, the protons required to complete reduction of O_2 to water would be taken from the negatively charged inside (***N***-side) of the membrane. Such a vectorial arrangement of the oxygen reduction chemistry of cytochrome *c* oxidase has been shown to be correct (Fig. 1), but it accounts for only one half of the energy transduction efficiency. 40 years ago it was discovered (2) that cytochrome *c* oxidase is actually a proton pump, in such a way that the redox loop function is complemented by translocation of one additional proton (per transferred electron) all across the membrane (Fig. 1) thus doubling the energy transduction efficiency. In terms of molecular mechanism this is a serious complication, mainly because a true proton pump requires kinetic gating functions that are unnecessary in a redox loop. Although the proton pump concept of cytochrome *c* oxidase was initially disputed for 8 years (3,4) it was a thermodynamically feasible proposal because the driving force, i.e. the difference in redox potentials between donor (cytochrome *c*) and acceptor (oxygen/water), is ca. 550 mV (5), which is more than enough to drive the equivalent of two protons across a membrane with a maximum pmf of ca. 220 mV. Moreover, cytochrome *c* oxidases from a

number of aerobic bacteria were also found to be proton pumps (see e.g. refs. 6-8), as was indeed the structurally homologous quinol oxidase, cytochrome bo_3, from *E. coli* (9). Further studies of the bacterial and archaeal worlds revealed that cytochrome *c* oxidase, originally mainly studied in mitochondria, was actually member of a very large superfamily of heme-copper oxidases (10). This family has been categorised in groups A (A1 and A2), B and C on the basis of structure, of which the A1 category is the only one in the mitochondria of eukaryotic cells, but also present in many aerobic bacteria.

In this paper we briefly review the main features of the proton-pumping mechanism of cytochrome *c* oxidase of type A1. Heme-copper oxidases of other types will be mentioned only when a comparison is warranted.

2. The catalytic cycle

All heme-copper oxidases have as a common feature an active site, called the binuclear center (BNC), comprised of a heme and a copper ion (Cu_B) close to the heme iron on the distal side (Fig. 2). Another feature common to these enzymes is that one of the three histidine ligands of Cu_B is covalently bonded to a tyrosine residue (Fig. 2). In Type A1 heme-copper oxidases the heme is usually heme A (called heme a_3 when bound to the protein), but in the quinol oxidase from *E. coli* it is heme O (heme o_3 when bound to the protein), which differs from heme A only by having a methyl group instead of a formyl in position 8 of the heme porphyrin ring, and hence quite different optical spectral properties (11).

Only the ferrous-cuprous form (state R) of the BNC is capable of binding O_2 onto the distal axial position of heme a_3, presumably because if the Cu_B is oxidized (cupric) it is likely to have a fourth oxygenous ligand in a position that prevents O_2 diffusion into binding distance of the heme iron (Fig. 3). O_2 binding is quite reversible (K_D ~0.28 mM at room temperature (12)) in contrast to the enzyme's high physiological affinity for oxygen (submicromolar range (13)). The reason for this paradox is trapping of the bound oxygen by fast electron transfer (13-15). The R state is best described as a ferric-superoxide adduct (13) even though it is often depicted as Fe[II]-O_2.

After O_2 binding the BNC catalyses a remarkable, "concerted", four-electron reduction of the bound dioxygen to the redox equivalents of water. We say "concerted" because until very recently no intermediate has been found experimentally, including no reactive oxygen species. However, quantum chemical density-functional theory calculations (16) have suggested an intermediate with bound peroxide, and recently, Brzezinski et al. (17) found

kinetic evidence for such an intermediate in the B-type cytochrome oxidase *ba*$_3$ from *Th. thermophilus*. From an oxidoreduction point of view, the two formed equivalents of water are an oxo group bound to a ferryl heme (Fe[IV]=O), and a hydroxyl group bound as a fourth ligand to the nearby copper (Fig. 3). The fourth reducing equivalent derives either from heme *a* or, in the case heme *a* is oxidized, from the conserved tyrosine residue that is covalently bonded to one of the three histidine ligands of Cu_B. The former state of the BNC has been called P_R, the latter P_M. In both cases the proton required for splitting the O-O bond derives from the conserved tyrosine (18).

The next experimentally observed intermediate is state F, which is at the same redox level as state P_R, but with an additional proton in the BNC. The OH^- ligand of Cu_B in the P_R state (19) is protonated to water, which probably dissociates from the copper (20,21) thus leaving the cupric Cu_B three-coordinate (and hence high potential). A high redox potential of Cu_B in this state is supported by DFT calculations, which indicate that this state has the ferryl heme and a mixture of Cu[II]-tyrosinate and Cu[I]-tyrosine neutral radical (21,22).

Reduction and protonation of the F state yields the ferric/cupric form of the BNC (state O), which is the state in the ”as isolated” enzyme. However, state O is almost certainly not catalytically active but is a relaxed product of an ”active form”, which has been termed O_H. O_H has been observed experimentally by Rousseau et al. (23) due to its resonance Raman Fe-O vibration at 450 cm^{-1}. The very low frequency of this vibration, compared with many other ferric-OH^- heme systems, made the authors suggest that the OH^- ligand is strongly H-bonded forcing the ferric heme to be high spin despite the strong-field axial ligand. Based on DFT calculations, we have proposed that this strong bonding exerted on the Fe-bound OH^- group may be due to a μ-hydroxy bridge between the iron and the copper (21, see also 22). Such a structure had been long predicted from chemical mimics of the binuclear site by Karlin et al. (24). The life-time of state O_H is uncertain since its decay in the Raman experiments could also be only apparent due to exchange of ^{18}O-labelled OH^- with $^{16}OH^-$.

Reduction (and protonation) of the O_H state has been studied by the electron injection technique, and the result has been a state (E_H) where a high-potential form of Cu_B (in state O_H) has been the sole electron acceptor (25). In equilibrium conditions, however, a single electron added to state O is roughly equally distributed between the two hemes and Cu_B (13, 26).

2.1. Electrical charge in the catalytic cycle

It is perhaps not unexpected that the overall electrical charge of the BNC is zero, considering that the center is located well within the phospholipid membrane. Taking state R as an example, the charge of the core of heme a_3 is zero because the porphyrinate^{2-} anion is neutralized by the ferrous (Fe^{2+}) heme iron. Cu_B[I] has a +1 charge, which is compensated by the -1 charge of the heme a_3 propionate A. (Propionate D (heme a_3) is charge-compensated by forming a salt pair with a conserved arginine residue).

The electroneutrality of the active site (BNC) is strictly adhered to, as first emphasized by Peter Rich (27,28), and is an extremely important property that is, in fact, central to the proton pump mechanism (see below). It is therefore of particular importance to note that there is one experimentally observed intermediate of the catalytic cycle that does not seem to follow the principle of electroneutrality. This is the state P_R (see above; Fig. 4). Fortunately, the structure of this state is quite well established (13,19). The ferryl heme (Fe[IV]=O; overall charge = zero) is accompanied by Cu[II]-OH^- and tyrosinate^{-1}; overall charge = zero). The negative charge of the heme a_3 propionate A (see above) is apparently not compensated. Evidence from electrometric experiments involving mutation of the conserved glutamic acid, glu-242, was interpreted to show that the formation of the P_R state from state A is accompanied by proton transfer from glu-242 to a ”pump site” or a ”proton-loading site” (PLS) on the **P**-side of heme a_3 in the vicinity of prpA of heme a_3 (5,29), i.e. by loading the PLS. This interpretation agrees very well with the expectation that the electroneutrality rule should be valid also in the case of intermediate P_R, as well as with the independently proposed location of the PLS (30-35).

3. The proton pump

Fig. 5 summarises the most entertained basic mechanism of the proton pump of cytochrome *c* oxidase (see e.g. ref. 13). Although there are four reactions of the catalytic cycle that each link to pumping of one proton, the basic mechanism appears to be the same at least for the two of the steps that have been best studied, viz. A→F and O_H→E_H. The loading of the PLS is coupled to the electron transfer from heme *a* to the binuclear site (BNC;13,29; I→II in Fig. 5). Whilst the chemical identity of the PLS is not known with certainty, most experimental and theoretical analyses suggest that it may be the A-propionate substituent of heme a_3, or residues in its immediate vicinity (30-35; cf. above). This location is supported by the generally accepted notion that the proton pump of cytochrome oxidase is a Coulombic solid state device that does not involve long-range

conformational changes. The loading of the PLS is followed by proton transfer to the BNC (state III, Fig. 5). The neutralization of the BNC lowers the pK_a of the PLS, and as a result the PLS proton is ejected to the ***P***-phase. In the following we will briefly outline the principles of this mechanism and, in particular, discuss how that mechanism is protected from back-leakage of protons from the ***P*** to the ***N*** side of the membrane.

3.1. Mechanistic principles

There is the completely conserved feature that the binuclear center (BNC) is accompanied by a low-spin heme in the immediate vicinity, at nearly v.d. Waals distance. This guarantees extremely fast electron transfer (eT) from heme *a* to the BNC (time constant ~1 ns; 36,37) as expected by the Moser-Dutton ruler (38). This fact, in turn, means that any restrictions observed on reaction rates in the various steps of catalysis are caused by other factors than eT, by proton transfer (pT) in particular. In practise, this means that *kinetic* gating of the proton pump which, as we shall see, is essential for it to work, cannot be achieved by controlling eT. However, eT is clearly regulated by the *thermodynamics* of the system, which often provides the linkage to protons and protonation. For example, after electron injection into Cu_A using a photosensitive dye (see e.g. 25) there is eT from Cu_A further to heme *a* in less than 25 μs, as expected from pure electron tunneling over that distance. However, there is no reduction of heme a_3 in this time domain even though the expected time constant (inverse rate constant) of eT between the hemes is ca. 1 ns (36,37). The reason is thermodynamics. The midpoint redox potential ($E_{m,7}$) of heme a_3 is far lower than that of heme *a on this time scale*, and hence fast eT from the latter to the former is countered by even faster eT in the reverse direction. The system literally waits for a proton to be placed near heme a_3 (or the BNC in general) thereby raising the $E_{m,7}$ to allow the eT to occur to a significant extent. The protonation thus gates the overall proton-coupled electron transfer, which takes place at the rate determined by the proton transfer.

The proton-pumping events are initialized by reduction of the electron donor, heme *a*. Differently from some previous interpretations, heme *a* reduction is not as such linked to protonation of the PLS (see 13), which is a concerted electron and proton transfer event (proton-coupled electron transfer, PCET), in which the electron moves from heme *a* to the BNC (Fig. 5, I→II). This implies that with heme *a* reduced the pK_a of the PLS is not high enough to accept a proton from the pH of ~7 of the aqueous ***N***-phase, and that the electron must move further to the BNC for this pK_a rise to occur, and for the proton to cross the

activation barrier (TS1 in Fig. 6). This further supports the location of the PLS to be close to the BNC (and further away from heme *a*).

Loading of the proton pump (the PLS) is thus a purely Coulombic event, and creates a dipole in which the positive charge of the proton in the PLS counter-balances the negative charge of the electron in the BNC, but does not annihilate it.

The next event is proton transfer from the reprotonated glu-242 to the BNC to complete the oxygen reduction chemistry (hence this proton is often called a ”chemical” proton). This results in annihilation of the electron charge in the BNC and hence in loss of the aforementioned dipole. As a result, the pK_a of the PLS is lowered back to its original value and the PLS proton is ejected to the aqueous ***P***-phase (Figs. 5,6). The pump action is completed, but why did the proton not rather go to the ***N***-side of the membrane as thermodynamics would have predicted (see Fig. 6, dashed orange arrow)? Again, we have a case where kinetic gating is essential in order to make such a mechanism work (see below).

3.2. Watergate mechanism revisited

One key problem of the pump mechanism is why, in the case the electron resides on heme *a*, there is no proton transfer to the binuclear site from glu-242 (and the D-channel). If that occurred, accompanying electron transfer from heme *a* to the BNC could not be avoided, and the chemistry of that particular partial reaction would be completed with no means to drive the proton pump. Brzezinski and Larsson (39) suggested an alternative where the uptake of the chemical proton is primary, and results in excited conformational states that relax with proton pumping, but this possibility has been made unlikely by experiments (see ref. 5).

The original watergate proposal (40) suggested that proton transfer to the BNC would not occur because, due to the electric field between heme *a* and the BNC, the water molecules in the cavity ”above” glu-242 would be orientated to allow proton transfer to the PLS (via the D-propionate of heme a_3), but disallowing proton transfer to the BNC. The latter would be allowed only after the electron transfer to the BNC and a switch of the direction of the electric field. This idea was criticized by Siegbahn and Blomberg (41) on the basis that the effect of the electric field on the orientation of the water dipoles would not be strong enough, and by Cui et al. (42, and citations therein), who instead emphasized control via hydration and dehydration of the apolar cavity. Control by hydration/dehydration of the

cavity as a result of the electric field was also thoroughly discussed by Kaila et al. (5). Multiscale reactive molecular dynamics simulations by Liang et al. (43) showed that proton transfer from glu-242 to the BNC has a high kinetic barrier in the state where the electron is still at heme *a*, but the molecular reason for this all-important barrier has remained unknown.

Recently, based on state-of-the-art metadynamics simulations as well as Markov state modeling, Son et al. (42) showed that the hydrophobic cavity hydrates (6-10 water molecules) when the D-propionate of heme a_3 is protonated. In contrast, it remains relatively dry with up to 1-3 water molecules, when the D-propionate is anionic. The D-propionate must be protonated at some point during proton migration from glu-242 to the PLS, but only transiently, which is consistent with the data that shows that the proton on the D-propionate is unstable and escapes to the A-propionate of heme a_3 (35). We think it is likely that classical modeling of a protonated D-propionate creates excessive hydration of the cavity and leak-like situations. Indeed, in a thoroughly hydrated cavity it is difficult to envisage how a proton on the protonated D-propionate would not leak back to the BNC, or to glu-242. In agreement with this view, Liang et al. (35) also see excessive hydration of the hydrophobic cavity when a proton is near the D-propionate of heme a_3.

The simulations by Son et al. (42) showed that the cavity runs relatively dry with 1-3 water molecules in the state with the electron at heme *a*. Interestingly, in the data presented in the article (also discussed briefly in SI and in a video), it appears that in this redox state a water-based connection to the BNC is not sufficiently populated, thereby partly supporting the water-gated model. They also observed that the water molecules exit the cavity on a tens of nanoseconds time scale, which may be sufficient for a rapid proton transfer from glu-242 to PLS, either concerted or as a charge separation. Finally, it is worth keeping in mind that turnover at the BNC produces two water molecules per cycle, which are most probably expelled into the hydrophobic cavity.

We repeated the original watergate MD simulations with the membrane-embedded protein (44) and we still found the original orientational effect on the water molecules in the cavity depending on the position of the electron. However, the preferential orientation of the water molecules accounts for an effect of only ca. 100-fold (~3 kcal/mol), so it could hardly alone explain the high efficiency of the proton pump. We envisage that water-based gating of protons to the PLS functions best in relatively dry conditions when there are 2-3

water molecules in the cavity and when the hydrophobic ceiling of the cavity (trp-126) is not entirely displaced due to expansion of the cavity, because 2-3 water molecules are sufficient to form the path from glu-242 to the D-propionate of heme a_3.

Considering the electric field in the apolar cavity domain between the hemes (Fig. 7) may give some further insight. Preliminary calculations (see ref. 5) have suggested that this electric field can be of the order of 1V/nm (i.e. 10^7 V/cm!). Transfer of a proton from glu-242 to the BNC via water would presumably start with formation of a charge-separated transition state where glu-242 would be negatively charged and a water molecule located between glu-242 and the BNC would be protonated to a hydronium ion. With the electron on heme *a*, i.e. prior to electron transfer to the BNC, the direction of such a dipolar transition state would be opposite to the direction of the electric field (Fig. 7), and hence expected to lie high in energy. In contrast, transfer of the proton from glu-242 to the PLS via the D-propionate of heme a_3 would be perpendicular to the field, and unaffected by it (see below). Thus, apart from the relative lack of water molecules between the glu-242 and the BNC, and their predominantly unfavourable orientation prior to electron transfer (40,44), the local electric field would be expected to make the proton transfer to the BNC very slow in this state and thus provide an efficient kinetic barrier against decoupling of the pump.

3.2. Other gating principles

As illustrated in Fig. 6., the ejection of the proton from the PLS due to lowering of its pK_a value is a serious cause of concern. With an unchanged energetics profile, the proton would undoubtedly flow back to the ***N***-side, i.e. across the lowest activation barrier (Fig. 6, orange dashed arrow). The barrier in the forward direction (from PLS towards the ***P***-side, TS2, Fig. 6) cannot be lowered either in order to compete, because then the barrier from the aqueous ***P***-side back to the PLS would become low enough to occupy the PLS from the wrong side. As originally stressed by Siegbahn and Blomberg (30) in their eminent analysis of leaks of the proton pump, this is the natural reason for why the rate of proton ejection from the PLS must be a slow event.

This analysis leads to the definite conclusion that the barrier for loading the PLS (TS1, Fig. 6) cannot remain the same after the loading has been completed, as first concluded by Siegbahn and Blomberg (30), and independently by Kim et al. (45) based on mathematical modelling of the proton pump. The obvious question, then, is what it is that keeps the barrier low for pT from glu-242 to the PLS as long as the electron is still at

heme *a*, but raises it considerably (30,45) when heme *a* is oxidized and the PLS is loaded (see below).

In 2008 it was proposed that the glu-242 residue may function as a valve of the proton pump due to observed kinetically asymmetric transitions between an ”up” position facing the apolar cavity, and a ”down” position facing the D-pathway in MD simulations (46). This function of the glutamic acid has been criticized. The earlier report by Yang and Cui (48), in which these observations were not confirmed, employed a structure of the BNC (P_R state) with the covalently bonded tyrosine neutral and protonated (contrast Fig. 3). In a more recent study (42) the authors emphasized states where they have protonated the heme a_3 propionate D, in an attempt to simulate a transient state during the transfer of the pumped proton from Glu242 to the PLS. This procedure leads to extensive ”wetting” of the apolar cavity and a preference of the negatively charged glu-242 carboxylate to be positioned ”upwards” facing the wetted cavity. Our earlier work on the glutamate ”gate” was criticized (42) on the basis that we used the compact cavity with only very few water molecules, indicated by the crystal structures, instead of an expanded cavity full of water. In our view, the latter condition is intolerable for the mechanism, because of direct protonic contact from the ***P***-side to the D-channel via such a multitude of water molecules, and resulting proton leakage. In our view the life-time of a protonated D-propionate (heme a_3) is too short to allow such an invasion of water into the nonpolar cavity, and to its dramatic extension in volume.

It is clear from the above (30,41,45,47) that there must be a considerable rate enhancement for pT from glu-242 to the PLS in the case prior to electron transfer compared to the case after eT (TS1 in Fig. 6). A change in barrier height of 7-8 kcal/mol was predicted, which is more than what seems achievable from the orientation and/or occupancy of water molecules, or from the gating function of glu-242. Siegbahn and Blomberg (30,41) have proposed an ingenious mechanism for this particular gating, viz. that the transition state is positively charged and hence lies low in energy when the electron in heme *a* stabilizes it electrostatically (TS1, Fig. 6). This stabilization is lost after the electron has been transferred to the BNC, and neutralized by the substrate proton. As a result the barrier rises considerably preventing proton leakage. This is a plausible mechanism, and is in accordance with the electric field between heme *a* and the BNC (Fig. 7), as the proton motion from glu-242 to the PLS via the D-propionate of heme a_3 will be perpendicular to this field.

4. Conclusions

We conclude that the structural interconversions of the binuclear heme-copper center (BNC) during the catalytic cycle of O_2 reduction to water are quite well understood at this point. The structure of the active O_H state is now also fairly well established based on Raman data, as complemented by both quantum-chemical simulations and by synthetic organometallic mimics. The reasons for why the active state is not occupied in cytochrome oxidase preparations, ”as isolated”, remain unclear. One possibility is that the apolar cavity loses its water molecules when the enzyme does not turn over, as is the case in all crystal structures. In such circumstances there would be no fast electron transfer beyond the low-spin heme, because in the absence of cavity water there is no accompanying proton transfer path beyond glu-242.

The mechanism of proton pumping is fairly well understood, but there are still uncertainties in some details, such as the precise location of the proton loading site (PLS), and the path of proton exit from the PLS to the ***P***-side of the membrane. Even if the PLS turns out to be more diffuse and not a single residue (such as the A-propionate of heme a_3), its location and the exit proton path are not trivial. There must be a high kinetic barrier against proton transfer from the aqueous ***P***-side to the PLS, high enough to prevent such pT even at a high protonmotive force (Fig. 6). At this time we do not have a good mechanistic/structural explanation of how this requirement is fulfilled. The mechanistic principles by which the pump avoids leakage, maintaining high efficiency even at fairly high loads of the protonmotive force, are indeed challenging also more generally, but beginning to be understood. One such mechanism ensures fast proton transfer from the ***N***-side of the membrane to the PLS as long as it is accompanied by electron transfer from heme *a* to the BNC. However, as soon as this proton-coupled electron transfer has occurred, the barrier for proton transfer to the PLS is drastically raised in order to prevent the proton in the PLS to diffuse back to the glu-242 (and further either back to the ***N***-side, or to be consumed at the BNC), instead of being ejected to the ***P***-side.

Finally, there must be mechanistic means to prevent premature proton transfer from the ***N***-side to the BNC that completes the oxygen reduction chemistry, bypassing proton pumping. The strong electric field between heme *a* and the BNC prior to the primary proton-coupled electron transfer indeed tends to orientate the water molecules in the apolar cavity to oppose such proton transfer, and to facilitate proton transfer to the PLS.

This orientational effect may not account for more than a ca. 100-fold preference of one pathway over the other. Here, we point out that the electric field may exert a much stronger controlling effect by raising the energy level of the transition state for proton transfer from glu-242 to the BNC.

REFERENCES

1. Mitchell, P., Chemiosmotic coupling in oxidative and photosynthetic phosphorylation, Biol. Rev., 41 (1966) 445-502,
2. Wikström, M.K., Proton pump coupled to cytochrome c oxidase in mitochondria, Nature, 266 (1977) 271-273.
3. Moyle, J., Mitchell, P., Cytochrome *c* oxidase is not a proton pump, FEBS Lett. 88 (1978) 268-272.
4. Wikström, M., Casey, R., The oxidation of exogenous cytochrome *c* in mitochondria, FEBS Lett. 183 (1985) 293-298.
5. Kaila, V.R.I., Verkhovsky, M.I., Wikström, M. Proton-coupled electron transfer in cytochrome oxidase, Chem. Rev. 110 (2010) 7062-7081.
6. Van Verseveld, H.W.,Krab, K., Stouthamer, A.H., Proton pump coupled to cytochrome *c* oxidase in *Paracoccus denitrificans*, Biochim. Biophys. Acta 635 (1981)525-534.
7. Solioz, M., Carafoli, E., Ludwig, B., The cytochrome *c* oxidase of *Paracoccus denitrificans* pumps protons in a reconstituted system, J. Biol. Chem. 257 (1982)1579-1582.
8. Hosler, J.P., Fetter, J., Tecklenburg, M.M.J., Espe, M., Lerma, C., Ferguson-Miller, S., Cytochrome aa_3 of *Rhodobacter sphaeroides* as a model for mitochondrial cytochrome *c* oxidase, J. Biol. Chem., 267 (1992) 24264-24272.
9. Puustinen, A., Finel, M., Virkki, M., Wikström, M., Cytochrome *o* (*bo*) is a proton pump in *Paracccus denitrificans* and *Escherichia coli*, FEBS Lett. 249 (1989) 163-167.
10. Sousa, F.L., Alves, R.J., Ribeiro, M.A., Pereira-Leal, J.B., Teixeira, M., Pereira, M.M., The superfamily of heme-copper oxygen reductases: Types and evolutionary considerations, Biochim. Biophys. Acta, 1817 (2012) 629-637.
11. Puustinen, A., Wikström, M., The heme groups of cytochrome *o* from *Escherichia coli*, Proc. Natl. Acad. Sci. USA, 88 (1991) 6122-6126.

12. Verkhovsky, M.I., Morgan, J.E., Wikström, M. Oxygen binding and activation: Early steps in the reaction of oxygen with cytochrome *c* oxidase, Biochemistry, 33 (1994) 3079-3086.
13. Wikström, M., Krab, K., Sharma, V., Oxygen activation and energy conservation by cytochrome *c* oxidase, Chem. Rev. DOI: 10.1021/acs.chemrev.7b00664 (2018)
14. Chance, B., Saronio, C., Leigh Jr, J.S. Functional intermediates in reaction of cytochrome oxidase with oxygen, Proc. Natl. Acad. Sci. USA, 72 (1975) 1635-1640.
15. Verkhovsky, M.I., Morgan, J.E., Puustinen A., Wikström, M., Kinetic trapping of oxygen in cell respiration, Nature, 380 (1996) 268-270.
16. Blomberg, M.R.A., Siegbahn, P.E.M., Quantum chemistry applied to the mechanisms of transition metal containing enzymes – cytochrome c oxidase, a particularly challenging case, J. Comput. Chem., 27 (2006) 1373-1384.
17. Poiana, F., von Ballmoos, C., Gonska, N., Blomberg, M.R.A., Ädelroth, P., Brzezinski, P., Splitting of the O-O bond at the heme-copper catalytic site of respiratory oxidases, Sci. Adv., 3 (2017) e1700279
18. Gorbikova, E.A., Belevich, I., Wikström, M., Verkhovsky, M.I., The proton donor for O-O bond scission by cytochrome *c* oxidase, Proc. Natl. Acad. Sci. USA, 105 (2008) 10733-10737.
19. Morgan, J.E., Verkhovsky, M.I., Palmer, G., Wikström, M., Role of the P_R intermediate in the reaction of cytochrome *c* oxidase with O_2, Biochemistry, 40 (2001) 6882-6892.
20. Du, W.-G.H., Götz, A.W., Noodleman, L., A water dimer shift activates a proton pumping pathway in the $P_R \rightarrow$ F transition of ba_3 cytochrome *c* oxidase, Inorg. Chem., 57 (2018) 1048-1059.
21. Sharma, V., Karlin, K.D., Wikström, M., Computational study of the activated O_H state in the catalytic mechanism of cytochrome *c* oxidase, Proc. Natl. Acad. Sci. USA 110 (2013) 16844-16849.
22. Blomberg, M.R.A., Mechanism of oxygen reduction in cytochrome c oxidase and the role of the active site tyrosine, Biochemistry, 55 (2016) 489-500.
23. Han, S., Takahashi, S., Rousseau, D.L., Time dependence of the catalytic intermediates in cytochrome *c* oxidase, J. Biol. Chem., 275 (2000) 1910-1919.
24. Kim, E., Chufan, E.E., Kamaraj, K., Karlin, K.D., Synthetic models for heme-copper oxidases, Chem. Rev., 104 (2004) 1077-1134.
25. Belevich, I., Bloch, D.A., Belevich, N., Wikström, M., Verkhovsky, M.I., Exploring the proton ump mechanism of cytochrome *c* oxidase in real time, Proc. Natl. Acad. Sci. USA, 104 (2007) 2685-2690.

26. Wikström, M., Krab, K., Saraste, M. Cytochrome oxidase – A synthesis, Academic Press, London (1981)
27. Mitchell, R., Rich, P.R., Proton uptake by cytochrome c oxidase on reduction and on ligand binding, Biochim. Biophys. Acta, 1186 (1994) 19-26.
28. Rich, P.R., Towards an understanding of the chemistry of oxygen reduction, Aust. J. Plant. Physiol., 22 (1995) 479-486.
29. Belevich, I., Verkhovsky, M.I., Wikström, M., Proton-coupled electron transfer drives the proton pump of cytochrome *c* oxidase, Nature, 440 (2006) 829-832.
30. Siegbahn, P.E.M., Blomberg, M.R.A., Energy diagrams and mechanism for proton pumping in cytochrome *c* oxidase, Biochim. Biophys. Acta, 1767 (2007) 1143-1156.
31. Wikström, M., Verkhovsky, M.I., Mechanism and energetics of proton translocation by the respiratory heme-copper oxidases, Biochim. Biophys. Acta, 1767 (2007) 1200-1214.
32. Sugitani, R., Medvedev, E.S., Stuchebrukhov, A.A., Theoretical and computational analysis of the membrane potential generated by cytochrome *c* oxidase upon single electron injection into the enzyme, Biochim. Biophys. Acta, 1777 (2008) 1129-1139.
33. Lee, H.J., Öjemyr, L., Vakkasoglu, A., Brzezinski, P., Gennis, R.B., Properties of Arg481 mutants of the aa_3-type cytochrome *c* oxidase from *Rhodobacter sphaeroides* suggest that neither R481 nor the nearby D-propionate of heme a_3 is likely to be the proton loading site of the proton pump, Biochemistry, 48 (2009) 7123-7131.
34. Lu, J., Gunner, M.R., Characterizing the proton loading site in cytochrome *c* oxidase, roc. Natl. Acad. Sci. USA, 111 (2014) 12414-12419.
35. Liang, R., Swanson, J.M.J., Peng, Y., Wikström, M., Voth, G.A., Multiscale simulations reveal key features of the proton-pumping mechanism in cytochrome *c* oxidase, Proc. Natl. Acad. Sci. USA, 113 (2016) 7420-7425.
36. Verkhovsky, M.I., Jasaitis, A., Wikström, M., Ultrafast Haem-Haem Electron Transfer in Cytochrome *c* Oxidase, Biochim. Biophys. Acta, 1506 (2001) 143-146.
37. Jasaitis, A., Johansson, M.P., Wikström, M., Vos, M.H., Verkhovsky, M.I., Nanosecond electron tunneling between the hemes in cytochrome bo3, Proc. Natl. Acad. Sci. USA, 104 (2007)20811-20814.
38. Page, C.C., Moser, C.C., Chen, X., Dutton, P.L., Natural engineering principles of electron tunnelling in biological oxidation-reduction, Nature, 402 (1999) 47-52.
39. Brzezinski, P., Larsson, G., Redox-driven proton pumping by heme-copper oxidases, Biochim. Biophys. Acta, 1605 (2003) 1-13.

40. Wikström, M., Verkhovsky, M.I., Hummer, G., Water-gated mechanism of proton translocation by cytochrome *c* oxidase, Biochim. Biophys. Acta, 1604 (2003) 61-65.

41. Blomberg, M.R.A., Siegbahn, P.E.M., The mechanism for proton pumping in cytochrome *c* oxidase from an electrostatic and quantum chemical perspective, Biochim. Biophys. Acta, 1817 (2012) 495-505.

42. Son, C.Y., Yethiraj, A., Cui, Q., Cavity hydration dynamics in cytochrome c oxidase and functional implications, Proc. Natl. Acad. Sci. USA, 114 (2017) 8830-8836.

43. Liang, R., Swanson, J.M.J., Wikström, M., Voth, G.A., Understanding the essential proton-pumping kinetic gates and decoupling mutations in cytochrome *c* oxidase, Proc. Natl. Acad. Sci. USA, 114 (2017) 5924-5929.

44. Sharma, V., Enkavi, G., Vattulainen, I., Róg, T., Wikström, M., Proton-coupled electron transfer and the role of water molecules in proton pumping by cytochrome c oxidase, Proc. Natl. Acad. Sci. USA, 112 (2015) 2040-2045.

45. Kim, Y.C., Wikström, M., Hummer, G., Kinetic gating of the proton pump in cytochrome *c* oxidase, Proc. Natl. Acad. Sci. USA, 106 (2009) 13707-13712.

46. Kaila, V.R.I., Verkhovsky, M.I., Hummer, G., Wikström, M., Glutamic acid 242 is a valve in the proton pump of cytochrome *c* oxidase, Proc. Natl.Acad. Sci. USA, 105 (2008)6255-6259.

47. Kim, Y.C., Hummer, G., Proton-pumping mechanism of cytochrome c oxidase: A kinetic master-equation approach, Biochim. Biophys. Acta, 1817 (2012) 526-536.

48. Yang, S., Cui, Q., Glu-286 rotation and water wire reorientation are unlikely the gating elements for proton pumping in cytochrome *c* oxidase, Biophys. J., 101 (2011) 61-69.

FIGURE LEGENDS

Fig 1. A-type C*c*O from *Bos taurus*. The two catalytic subunits I and II are shown in blue and red transparent ribbons. The eT and pT paths are shown with red and blue arrows respectively, whereas substrate oxygen enters through the lipid milieu (black dotted lines) and product water is released to the ***P***-side (or to the ***N***-side) of the membrane. The D- and K-channels supply both 'pumped' and 'chemical' protons in bacterial oxidases, whereas the H-channel is controversial, but has been proposed to transfer all pumped protons in mammalian mitochondrial A-type oxidases (see ref. 13). Key amino acid residues are highlighted and shown in licorice representation, together with coppers (orange) and hemes (yellow).

Fig.2. Binuclear center. A view in the membrane plane. The three histidine ligands of Cu_B (orange) are indicated in blue, along with the covalently bonded tyrosine residue Y244. Heme a_3 is shown in yellow.

Fig. 3. Catalytic cycle. The square encompasses the binuclear center (BNC) consisting of heme a_3, Cu_B and the covalently bonded tyrosine residue (HO-tyr). The name of the intermediate is given above the upper right corner of each square. The frequencies of the iron-oxygen resonance Raman stretch is given for each intermediate (see ref 13). The uptake of ”chemical” protons is indicated. Proton pumping is not shown here, but is coupled to each one-electron reduction step. The P_R state is high-lighted because of its special status (see text).

Fig. 4. Charge neutralisation during conversion of state P_R to state F. The A-propionate of heme a_3 is indicated above the blue heme plane. Normally, and in all crystal structures, this propionate is unprotonated and receives a hydrogen bond from a conserved aspartic acid. This is the presumed proton-loading site (PLS, see text), and it is loaded in the P_R state (as shown in the figure), and unloaded in state F due to electrostatic repulsion from the incoming substrate proton.

Fig. 5. Basic proton pump mechanism. The symbols are defined in state I. PLS=proton-loading site. BNC=binuclear center. The key difference relative to some other related proposals is that loading the PLS is a proton-coupled electron transfer event that requires eT from heme *a* to the BNC, and does not occur as a result of heme *a* reduction.

Fig. 6. Simplified energy diagram of the pump mechanism. The reaction coordinate describes the motion of the pumped proton against a protonmotive force between the aqueous ***P***- and ***N***-phases. In the first step it moves from the ***N***-side of the membrane (via glu-242) to the PLS across the transition state TS1 together with the eT from heme *a* to the BNC. In the next step the pK_a of the PLS is lowered due to neutralization of the electron charge at the BNC by uptake of the ”chemical” proton. As a result, the PLS proton is ejected to the ***P***-side, across transition state TS2. The orange dashed arrow points out the requirement of kinetic gating; what prevents the PLS proton from diffusing back to the ***N***-side? (see text).

Fig. 7. Electric field in the apolar cavity. The blue arrow indicates the direction of the electric field of the order of 1 V/nm in the space between heme *a* and the BNC in the case where heme *a* is reduced and BNC is oxidized, i.e. prior to the proton-coupled electron transfer that loads the proton-loading site with a proton (see text).

Acknowledgements

MW gratefully acknowledges support from the Magnus Ehrnrooth Foundation and Societas Scientiarum Fennica. VS is thankful to the Academy of Finland and University of Helsinki for financial support, and to the Center for Scientific Computing (CSC, Finland) for long-term computational support.

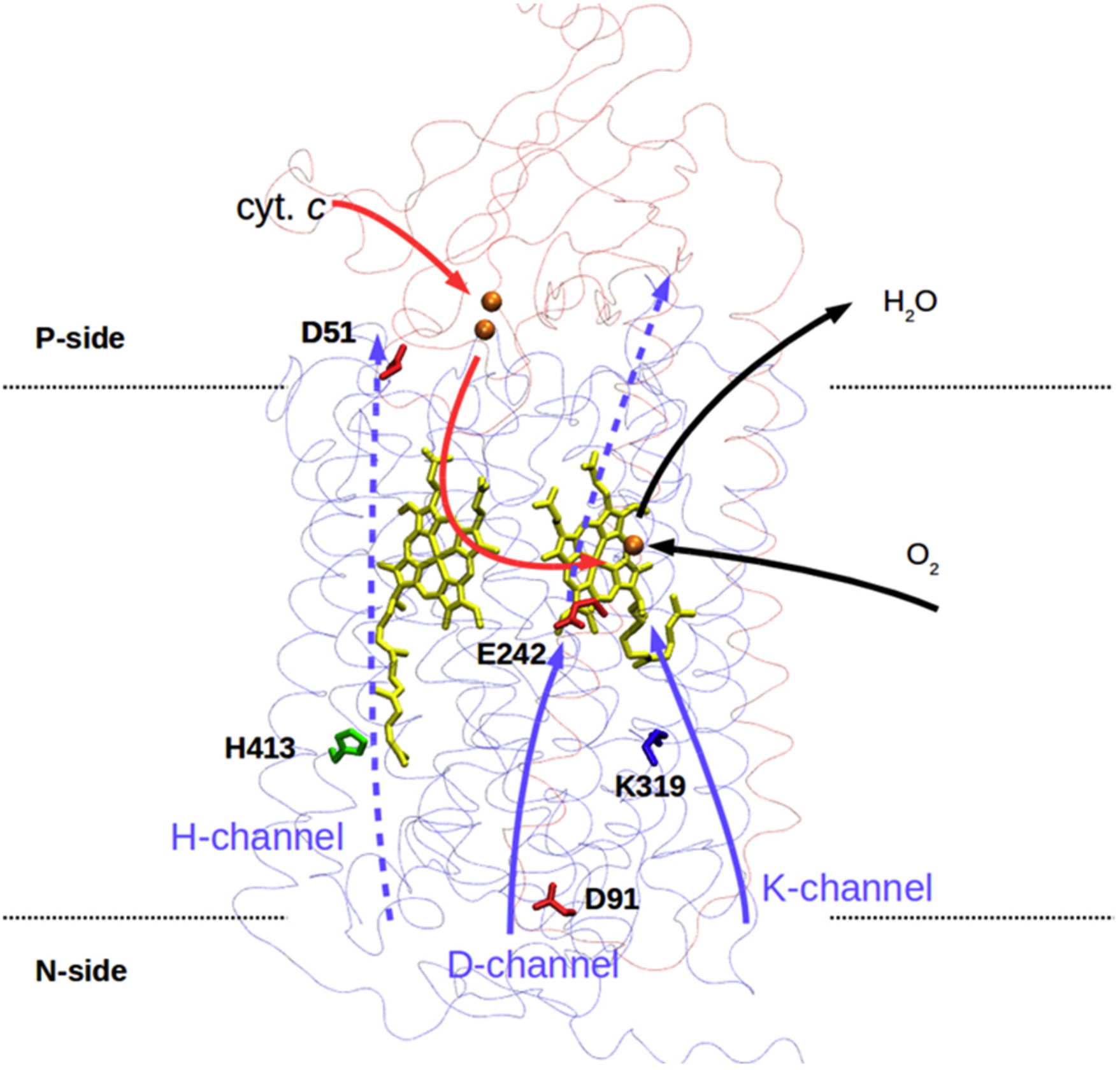
cyt. c
P-side
D51
H2O
O2
E242
H413
K319
H-channel
D91
K-channel
D-channel
N-side

Figure 1

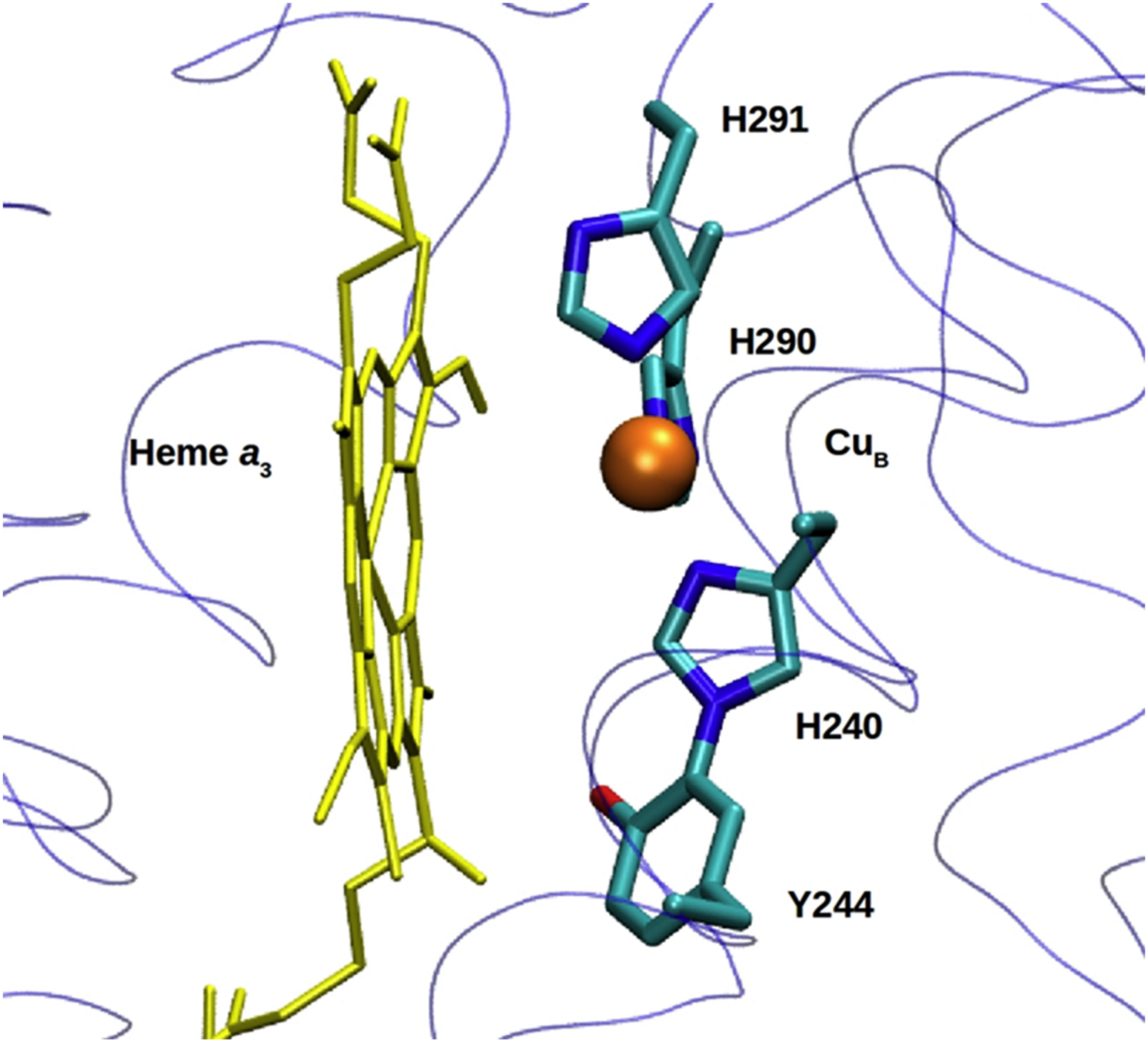

Figure 2

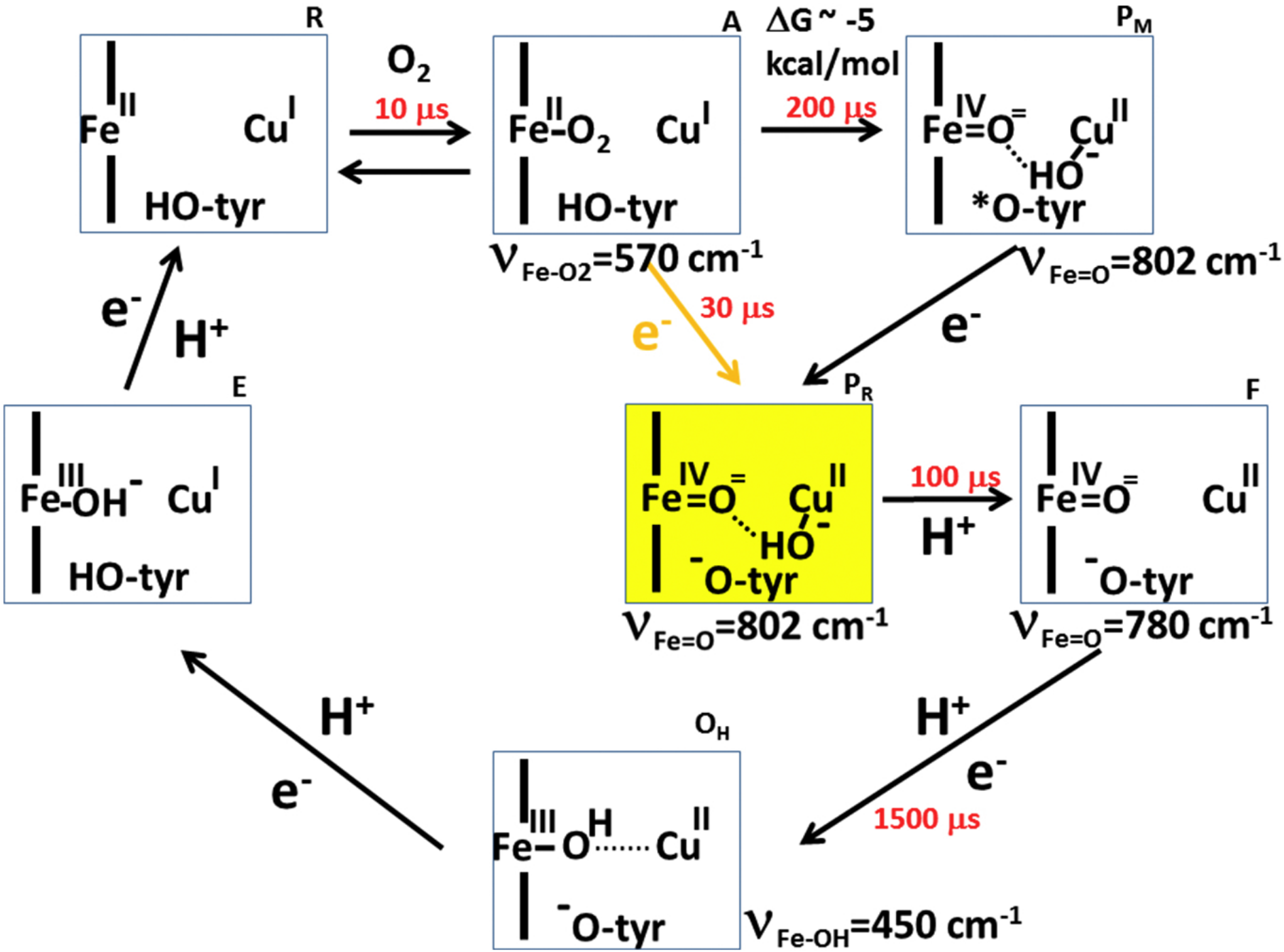
R
A
ΔG ~ -5 kcal/mol
P_M
O2
10 μs
200 μs
Fe^II
Cu^I
HO-tyr
Fe^II–O2
Cu^I
HO-tyr
Fe^IV=O^=
Cu^II
HO^-
*O-tyr
ν Fe-O2=570 cm-1
ν Fe=O=802 cm-1
e-
30 μs
e-
e-
H+
E
P_R
F
Fe^III–OH^-
Cu^I
HO-tyr
Fe^IV=O^=
Cu^II
HO^-
-O-tyr
100 μs
H+
Fe^IV=O^=
Cu^II
-O-tyr
ν Fe=O=802 cm-1
ν Fe=O=780 cm-1
H+
e-
O_H
H+
e-
1500 μs
Fe^III–O^H
Cu^II
-O-tyr
ν Fe-OH=450 cm-1

Figure 3

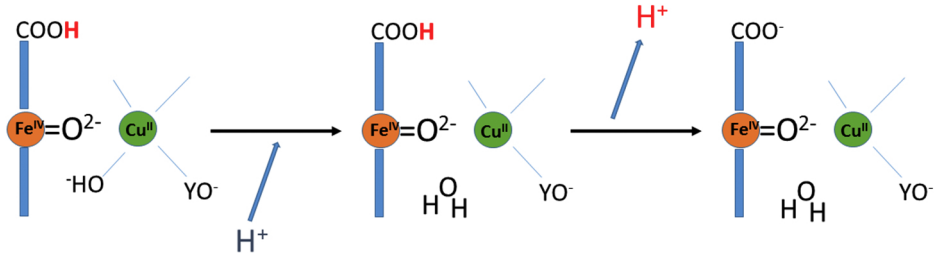

STATE	**P_R**	**transient intermediate**	**F**
CHARGE	**zero**	**+1**	**zero**

Figure 4

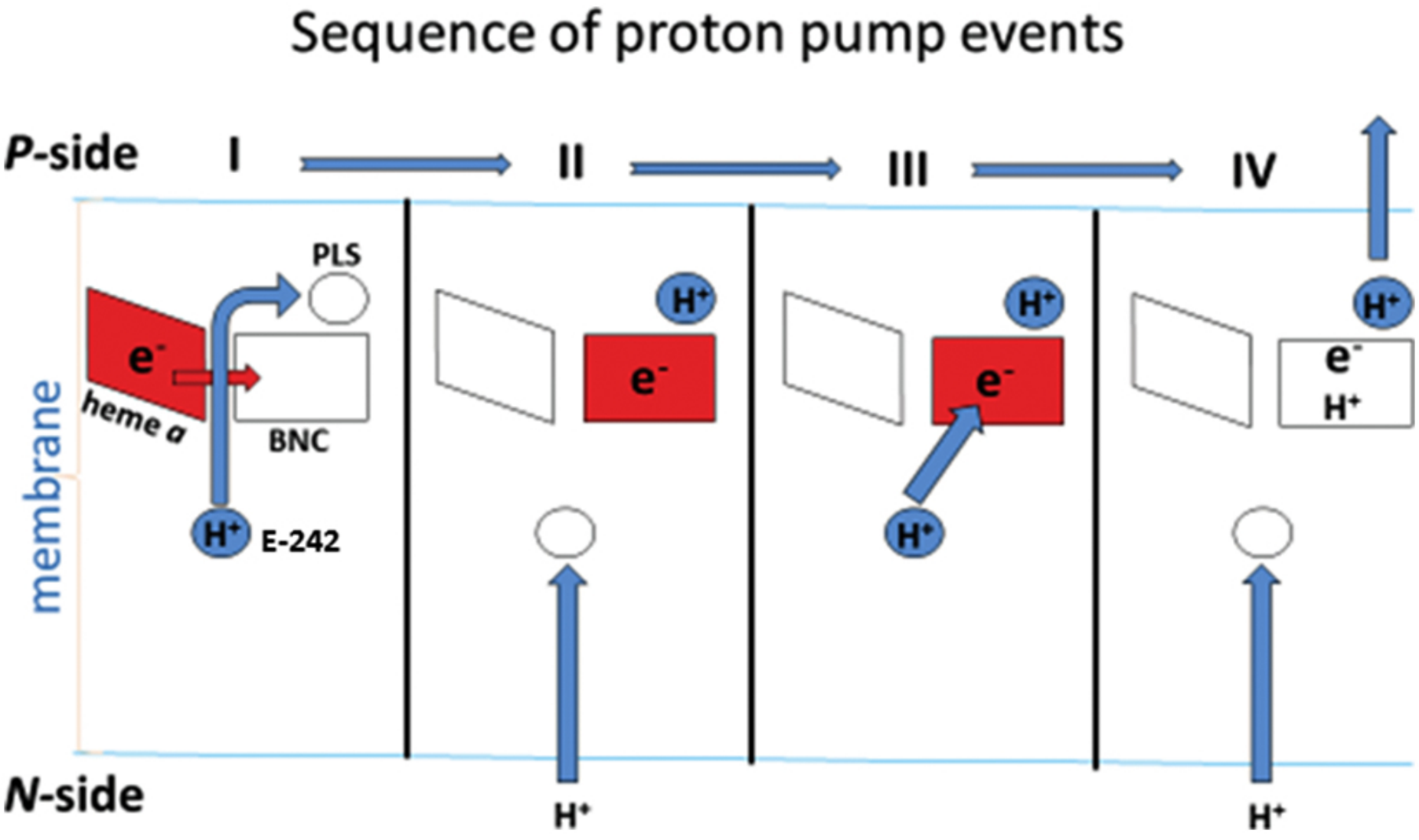
Sequence of proton pump events
P-side
I
II
III
IV
PLS
e-
heme a
BNC
H+
E-242
membrane
e-
H+
e-
H+
H+
e-
H+
H+
H+
N-side
H+
H+

Figure 5

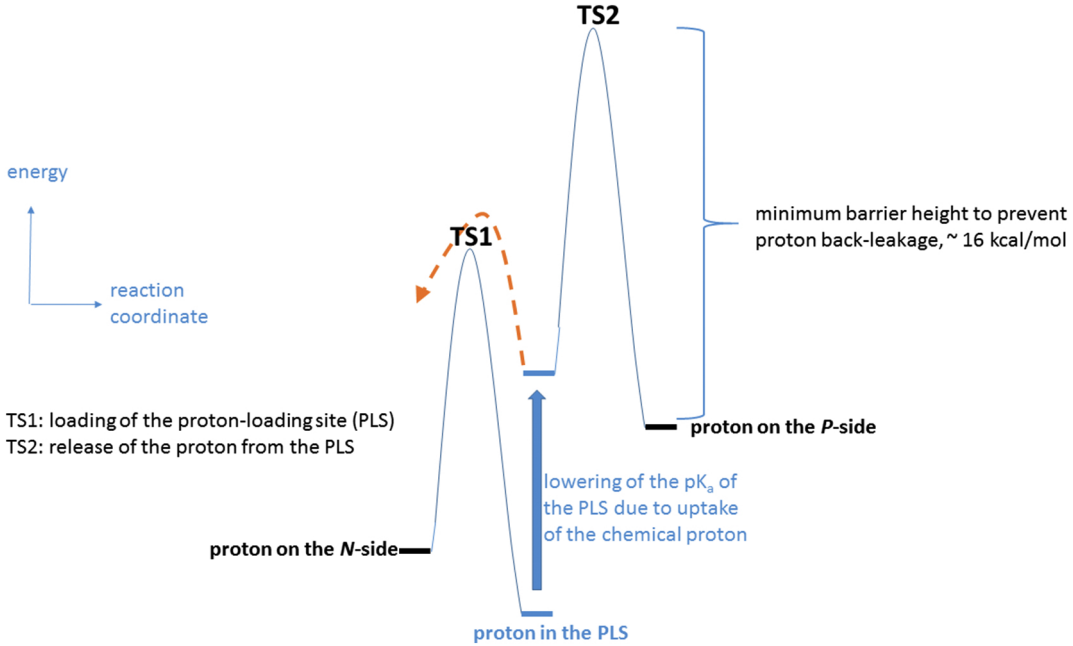
TS2
energy
TS1
minimum barrier height to prevent proton back-leakage, ~ 16 kcal/mol
reaction coordinate
TS1: loading of the proton-loading site (PLS)
TS2: release of the proton from the PLS
proton on the P-side
lowering of the pKa of the PLS due to uptake of the chemical proton
proton on the N-side
proton in the PLS

Figure 6

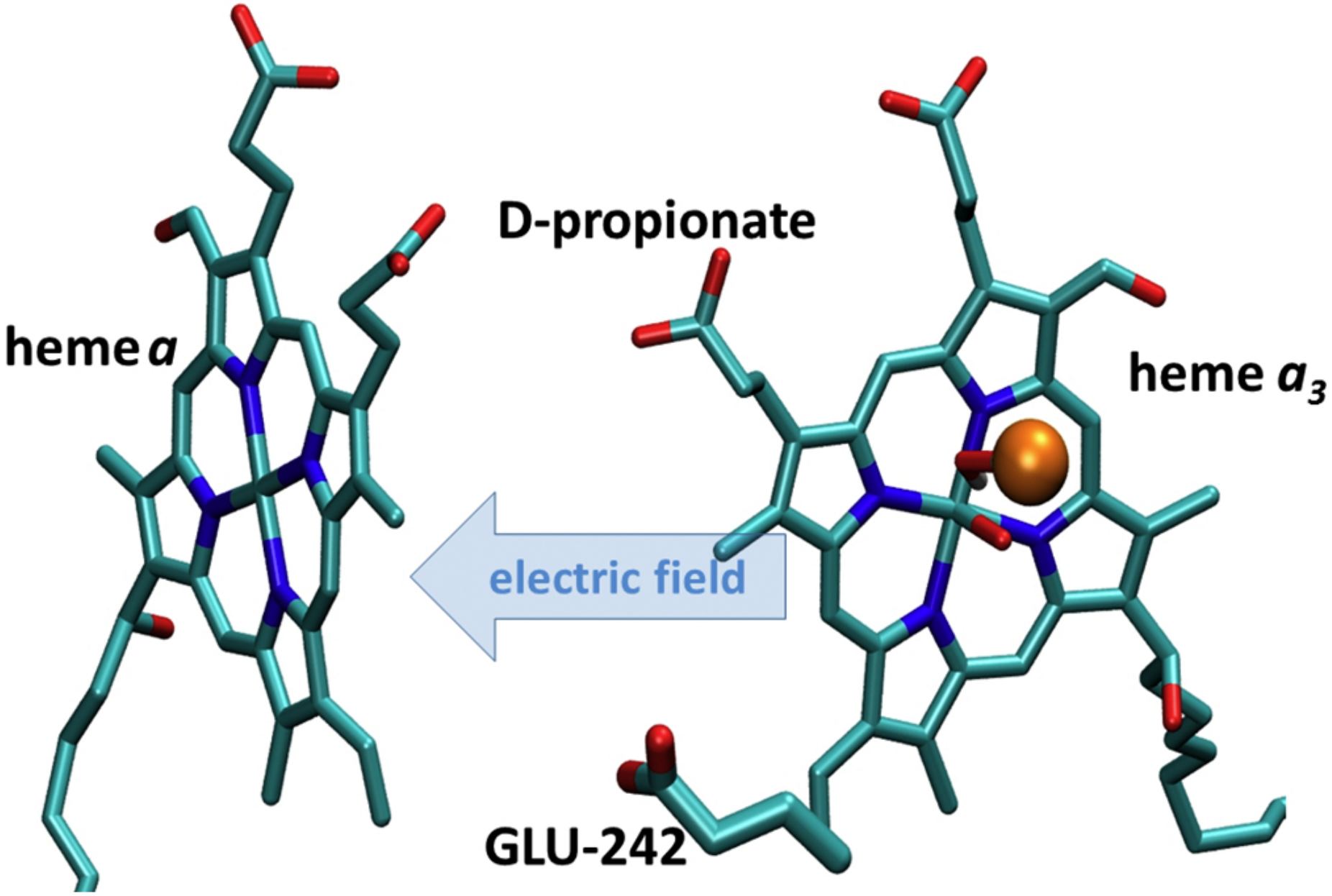

Figure 7